Istraživanja i projektovanja za privredu
ISSN 1451-4117
DOI:10.5937/jaes0-39723
www.engineeringscience.rs

iipp publishing

Journal of Applied Engineering Science
Vol. 21, No. 1, 2023
Original Scientific Paper
Paper number: 21(2023)1, 1059, 143-156

PREDICTIVE MODELS OF BEHAVIOR AND CAPACITY OF FRP REINFORCED CONCRETE COLUMNS

Yazan Momani[1]*, Ahmad Tarawneh[2], Roaa Alawadi[3], Ziad N. Taqieddin[4], Yazeed S. Jweihan[5], Eman Saleh[6]

[1] Assistant Professor, Civil Engineering Department, Faculty of Engineering, University of Petra, Amman, Jordan
[2] Assistant Professor, Civil Engineering Department, Faculty of Engineering, The Hashemite University, P.O. box 330127, Zarqa 13133, Jordan
[3] Assistant Professor, Civil Engineering Department, Faculty of Engineering, Applied Science Private University, Amman, Jordan
[4] Associate Professor, Civil Engineering Department, Faculty of Engineering, University of Petra, Amman, Jordan
[5] Assistant Professor, Civil and Environmental Engineering Department, Faculty of Engineering, Mutah University, Mutah, Karak, 61710, P.O. BOX 7, Jordan
[6] Assistant Professor, Civil Engineering Department, Faculty of Engineering, The Hashemite University, P.O. box 330127, Zarqa 13133, Jordan

** yazan.almomani@uop.edu.jo*

This paper proposes a new model for predicting the axial capacity and behavior of Fiber Reinforced Polymer-reinforced concrete (FRP-RC) columns using a promising variant of Genetic Expression Programming (GEP). Current design codes, such as the ACI 440.1R-15 and the Canadian Code CSA S806, disregard the compressive contribution of FRP bars when used in compression members. The behavior of concentrically short FRP-RC columns has been widely investigated in the past few years; however, limited research has been dedicated to investigating the effect of load eccentricity and the slenderness ratio of FRP-RC columns. In addition, the methodologies adopted for including the effect of column slenderness remain a subject of debate, as no solid conclusions are withdrawn in this regard. In this paper, the experimental results of FRP-RC columns are gathered from the literature and used to formulate two GEP models to predict the axial capacity based on load eccentricity. The experimental data includes columns reinforced with different FRP types and subjected to concentric and eccentric axial compressive loads. In addition, the database comprises short and slender columns. The proposed GEP models are functions of concrete compressive strength, longitudinal reinforcing bars ratio, FRP bars elastic modulus, eccentricity level, and column dimensions. For the aim of comparison, a preliminary evaluation of previously suggested empirical equations/models for estimating the axial capacity of FRP-RC columns was carried out over the collected database. The proposed models showed superior accuracy in axial capacity prediction with coefficients of determination R^2 equals to 0.978 and R^2 equal to 0.992 for eccentric and concentric axial load, respectively. The proposed models were found to give reliable estimates of the axial capacity of columns reinforced with FRP longitudinal bars. Finally, a parametric study to evaluate the effect of each variable on the proposed models was conducted.

Keywords: FRP composite bars, FRP-RC columns, slender columns, eccentric loading, Gene expression programming, machine learning

1 INTRODUCTION

Fiber Reinforced Polymer (FRP) composite bars have emerged through the years as an efficient substitute for conventional steel reinforcing bars, due to their exceptional corrosion resistance, as well as other advantageous properties. Conventional reinforced concrete (RC) structures deteriorate in harsh conditions due to the corrosion of the reinforcing steel [1]. FRP bars could result in significant cost savings when compared to the replacement or rehabilitation of deteriorated RC elements. FRP materials possess many characteristics that improve their performance as a reinforcement substitute: a low elastic modulus (in comparison to steel reinforcing bars), a high strength-to-weight ratio, and a linear stress-strain relationship [2]. FRP bars are composed of aligned fibers embedded in a resin matrix and have a brittle stress-strain curve with an elastic modulus that varies depending on the fiber's type. Concrete structural members reinforced with GFRP bars, for example, demonstrate superior durability and strength [3].

Over the past twenty years, extensive analytical and experimental investigations have been carried out to study the behavior of FRP-RC beams flexural and shear loads [3,4]. The outcomes of the research studies were used to establish design guidelines (ACI 440.1R-15 [5], CAN/CSA S806-12[6]) for FRP-reinforced flexural elements. Accordingly, FRP bars have been utilized in bridge girders and beams [4]. However, the design guidelines (ACI 440.1R-15 and CAN/CSA S806-12) related to the use of FRP in compression regions disregard the contribution of FRP bars in beams and columns, resulting in a conservative estimation of capacity, and thus paving the way for more research in this context. In this paper, genetic expression programming is utilized to introduce two models to simulate the axial capacity of FRP-RC columns loaded concentrically and eccentrically.

In this paper, two new GEP models are proposed to predict the axial capacity and behavior of FRP-RC columns. The required experimental data for short and long, concentrically and eccentrically loaded FRP-RC columns is gathered from the literature and used to formulate the two GEP models for columns reinforced with different types of fibers.

The genes influencing the performance of the GEP models are defined and analyzed, with a parametric study conducted to evaluate the effect of each variable on the proposed models. A comparison is carried out between the results obtained in this paper and those of empirical models previously suggested and available in the literature, where the results of the comparison indicate the superiority of the proposed models in determining the axial capacity of eccentrically and concentrically loaded FRP-RC columns.

2 PREVIOUS STUDIES

As was already indicated, the unpredictability in estimating that contribution causes the present design codes to ignore the compressive contribution of FRP bars in columns. Several studies were devoted to investigating the FRP bars' behavior in axially loaded columns. De Luca et al. (2010) studied the performance of concentrically loaded GRFP-RC columns. The study indicated that the behavior of GFRP-RC columns behaves similarly to typical steel-reinforced columns with just a little reduction in axial capacity when the reinforcement ratio equals one percent [7]. Alsayed et al. (1999) reported a thirteen percent reduction in axial capacity with direct replacement of longitudinal steel reinforcement with GFRP reinforcement, maintaining a similar reinforcement ratio [8]. By comparing many scientific contributions in the literature, there appears to be no mutual agreement regarding the determination of the FRP contribution in the column capacity. Elchalkani and Ma (2017) [9], Hadhood et al. (2017) [10], and De Luca et al. [7] measured the contribution of GFRP longitudinal bars within five percent of the column nominal compressive strength. Tobbie et al. (2012) [11]. and Afifi et al. (2014) [12] noticed that the steel reinforcement contribution is 12 percent, whereas the GFRP contribution is between 5 and 10 percent.

Guérin et al. (2018a) performed 12 large-scale GFRP-RC columns under a wide range of eccentricity levels. The study showed that the capacity and behavior of the GFRP in particular and the reinforced column, in general, were significantly affected by the eccentricity level. Additionally, the study discovered that, for the same amount of eccentricity, FRP-RC and steel-RC columns behaved similarly, with no discernible difference for the FRP manufacturer. When compared to standard steel-RC specimens, GFRP RC columns with eccentricity values ranging from 6 to 27 percent have a lower capacity, and a compression-ductile failure was the primary failure mechanism. [13]. Guérin et al. reported the contribution of GFRP bars as a function of the load eccentricity: on average, the load carried by GFRP bars was 3%, 5%, and 13% of peak load for specimens with low eccentricity (e / h = 0.1 to 0.2), moderate eccentricity (e / h = 0.4), and high eccentricity (e / h = 0.8), respectively.

Another experimental program was conducted by Guérin et al. (2018b) to investigate the contribution of the FRP reinforcement ratio to the performance and capacity of eccentrically FRP-RC columns. The results showed that increasing the reinforcement ratio from one to three percent increased the capacity by almost ten percent for columns with low eccentricity (e / h = 0.1 to 0.2) and 35% for columns with high eccentricity (e / h = 0.8). In addition, the parametric investigation revealed that the failure envelope considerably increased when concrete compressive strength raised from 30 to 60 MPa (approximately 100%). The study's results indicated that correct predictions are obtained when the GFRP's contribution in compression is taken into account [14].

Understanding the behavior of FRP-RC columns can be more complicated than steel-RC columns, particularly in the case of eccentric loading mainly due to the different contributing variables such as elastic modulus of FRP bars, concrete compressive strength, reinforcement ratio, slenderness ratio, and column dimensions for each experiment. The existing empirical models for the FRP-RC columns were built using regression analysis and a limited number of experimental data, therefore researchers were unable to account for all possible combinations and interrelations of the variables in order to create an accurate model (Raza et. al 2020) [15]. Furthermore, there is a lack of research studies when considering eccentric axial load and column slenderness in predicting the capacity of FRP-RC columns. Artificial intelligence techniques have seen great attention recently, as they are implemented to understand the complex nature of various phenomena and generalizations, by breaking down sophisticated mathematical relations into simple operations [16]. The utilization of artificial intelligence techniques has been extended to various applications in structural and civil engineering. For instance, Solhmirzaei et al. in 2020 developed a machine learning framework utilizing gene expression programming (GEP), an artificial neural network (ANN), and a large experimental database that is capable to predict strength and failure for ultra-high-performance concrete beams [17]. In 2021 Tarawneh et al. utilized GEP to develop a strength model for the shear capacity of steel-fiber-reinforced concrete based on a large experimental database [18]. The developed model provided superior accuracy compared to other models proposed in the literature. In civil engineering applications, Imam et al. (2021) developed a Pavement Condition Index from International Roughness Index using Gene Expression Programming [19].

The higher accuracy achieved by machine learning tools and their ability in pattern recognition is very crucial in the design process for different reasons. First, developing a machine learning-based model is considered a faster and easier tool in developing robust models compared to simple regression that may not accurately account for some affecting variables. Secondly, an accurate model means a higher safety level. An accurate prediction model with a low coefficient of variation and standard deviation allows for increasing the strength reduction factor in the design process while maintaining the same safety level which is described by the reliability index. Finally, this will allow for better utilization and economic use for structural members.

This study utilizes a GEP technique to understand and predict the behavior of FRP-RC columns by considering the individual contribution and the effect of each of the column properties, such as reinforcement ratio, FRP bars elastic modulus, concrete compressive strength, eccentricity level, and column dimensions.

3 DATA-DRIVEN GENE EXPRESSION MODEL DEVELOPMENT

This section describes the development of the machine GEP model and surveyed experimental database.

3.1 Experimental Data

Any gene expression model that aims to learn, be able to recognize patterns, and forecast performance needs a data set for training. A survey and collection of experimental data on FRP-RC columns carrying concentric and eccentric loads has been done as a result. The data set consists of 247 experimentally tested columns with a variety of parameters, including eccentricity level(e/h), reinforcement ratio (ρ), FRP elastic modulus (E), concrete compressive strength (f_c'), and column dimensions ($b \times h$). An overview of the experimental data for concentric and eccentric FRP-RC columns is presented in Table 1.

Table 1 Experimental data gathered from the literature

Reference	No. of specimens	$b \times h$ mm	f_c' MPa	FRP Type	ρ %	e/h
Eccentrically loaded columns						
Hadhood et al. (2017) [10]	43	305x305	35-70.2	GFRP & CFRP	2.18-3.7	0.082-0.65
Xue et al. (2018) [20]	12	300x300	39-55.2	GFRP	1.3-2.6	0.2-1
Amer et al. (1996) [21]	4	150x150	32	CFRP	0.76	0.2-0.8
Sharbatdar (2003)[22]	5	230x230	54.1	CFRP	0.38	0.26, 0.33
Tikka et al. (2010) [23]	8	150x150	35.7	GFRP	2.3-3.4	0.2-0.8
Gong and Zhang (2009) [24]	10	180x250	24,29	CFRP	0.46-0.9	0.1-1.44
Elchalakani et al. (2018) [25]	6	260x160	26	GFRP	2.37	0.16-0.5
Khorramian and Sadeghian (2017) [26]	6	150x150	37	GFRP	5.33	0.1-0.3
Sun et al. (2017) [27]	9	180x250	26.8	GFRP	1.05	0.3-0.7
Guérin (2018 a) [13]	8	405x405	42.3	GFRP	1.1	0.1-0.8
Guérin (2018 b) [14]	8	405x405	42.3	GFRP	1.39-2.47	0.1-0.8
Elchalakani and Ma (2017) [9]	4	260x160	32.75	GFRP	1.83	0.16-0.22
Issa et al. (2012) [28]	2	150x150	24.73	GFRP	2.01	0.16,0.33
Othman et al. (2019) [29]	20	150x150	44.7	CFRP	1.4-3.6	0.5,1
Salah-Eldin et al. (2019) [30]	4	400x400	71.2	GFRP	1	0.2-0.6
Hadi and Youssef (2016) [31]	4	210x210	33	GFRP	1.15	0.12-0.24
Khorramian and Sadeghian (2019) [32]	1	305x203	48	GFRP	4.7	0.25
Abdulazim et al. (2020) [33]	15	305x305	46	GFRP	2.9-4.6	0.16-0.65
Khorramian and Sadeghian (2020) [34]	9	305x205	56.8	GFRP	2.8-4.8	0.207-0.2317
Concentrically loaded columns						
Xue et al. (2018) [20]	3	300x300	39	GFRP	1.34	0
Elchalakani and Ma (2017) [9]	3	260x160	33	GFRP	1.83	0
Khorramian and Sadeghian (2017) [26]	2	150x150	37	GFRP	5.36	0

Reference	No. of specimens	$b \times h$ mm	f_c' MPa	FRP Type	ρ %	e / h
Eccentrically loaded columns						
Elchalakani et al. (2018) [25]	3	260x160	26	GFRP	2.37	0
Othman et al. (2019) [29]	5	150x150	45	CFRP	1.4-3.6	0
Hadi and Youssef (2016) [31]	1	210x210	33	GFRP	1.15	0
De Luca et al. (2010) [7]	4	610x610	33-44	GFRP	1	0
Tobbi et al. 2012[11]	5	350x350	33	GFRP	187, 1.95	0
Maranan et al. (2016) [35]	2	250x250	38	GFRP	2.43	0
Elmesalami et al. (2021) [36]	3	180x180	34.4	GFRP	2.48-3.88	0
Abdulazim et al. (2020) [33]	10	305x305	46.6	GFRP	2.9-4.6	0
Mohammad et al. (2014) [37]	9	300x300	42.9	GFRP & CFRP	1.79-2.19	0
Afifi et al. (2014) [12]	9	300x300	42.9	GFRP	1.1-3.2	0
Hadhood et al. (2017) [10]	7	305x305	35-70.2	GFRP & CFRP	2.18-3.7	0

3.2 Gene Expression Programming

Typically, Gene Expression Programming (GEP) is a tool for finding the best mathematical expression using a random set of data that has been wildly used. In general, data used in GEP should consist of a number of inputs used to predict an output value. Each input represents a variable. The program generates several models which are potential solutions to the problem. The models are compared with the correlation coefficient R^2 and the Root-Mean-Square Error (RMSE). A variety of sized and shaped expression trees can then be used to depict the best model. The trees, known as GEP Expression Trees (ETs), may be represented as a mathematical function, as demonstrated in Fig. 1.

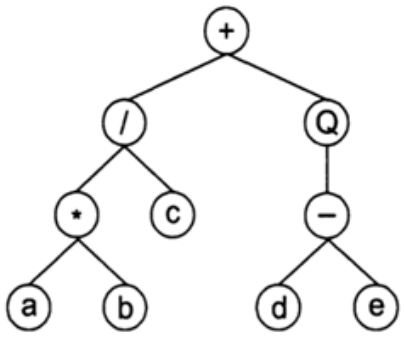

$$\frac{a.b}{c} + \sqrt{d - e}$$

Fig. 1. Tree expressions and corresponding mathematical expressions

Two GEP models are developed to study both concentric and eccentrically loaded columns. Concentrically loaded columns data set consists of 69 tests. The main database has been divided into two parts; Training dataset and validation dataset. Randomly divided, 46 data points (66.6%) were selected for the training dataset, and the remaining 23 data points (33.3%) were considered for the validation data set. On the other hand, for eccentric columns, the data set gathered from literature consists of 178 tests. Additionally, this entire data set is randomly split into training and testing data sets. For the training dataset, 118 data points (66.6%) were chosen at random, while the remaining 60 data points (33.3%) were taken into account for the testing dataset. Table 2 lists the parameters chosen for the GEP algorithm. The parameters were chosen after several testing. Criteria for choosing the parameters was based on several trials while tracking the coefficient of variation (COV), the average of the tested-

to-predicted ratio ($P_{tested} / P_{predicted}$), and the Root-Mean-Square Error (RMSE). In order to provide a straightforward model, only fundamental mathematical operations were chosen for the function set.

Table 2: GEP selected parameters

Parameter	*Selected value*
Dependent variable (axial load)	1
Independent variables	5
Genes	3
Function set	−, +, ×, ÷
Head size	4
The linking function between ETs	Addition

A training phase and a testing phase are involved in creating a gene expression model. In the training phases, the input information is entered in multiple mathematical processes and is adjusted to reduce the difference in inaccuracy between the input and output layers. Gene expression models evaluate error using RMSE. The training procedure is continued until the RMSE error has stabilized across a number of iterations.

4 PROPOSED GEP MODEL

The GEP algorithm discussed previously has been applied along with the experimental database to develop prediction models for concentrically and eccentrically loaded FRP-RC columns. The developed two GEP models are presented in form of expression trees as shown in Figures 2 and 3. The models consist of three sub-trees (ET) linked by addition for concentric loading and multiplication for eccentric loading. In the presented ET for concentrically loaded columns, d_o, d_1, d_2, d_3, and d_4 represent A, $f_c^{'}$, ρ, E, and *l*/*r*, respectively. While d_o, d_1, d_2, d_3, d_4 and d_5 represent A, e/h, $f_c^{'}$, ρ, E, and *l*/*r*, respectively, for eccentrically loaded columns. Table 3 provides a list of the constants in the gene expression tree. The concentric axial load model is fed by five given inputs, which are A, E, ρ, *l*/*r*, and $f_c^{'}$, to predict the axial load capacity. While the eccentric load model is fed by six given inputs, which are A, E, ρ, *l*/*r*, e/h, and $f_c^{'}$.

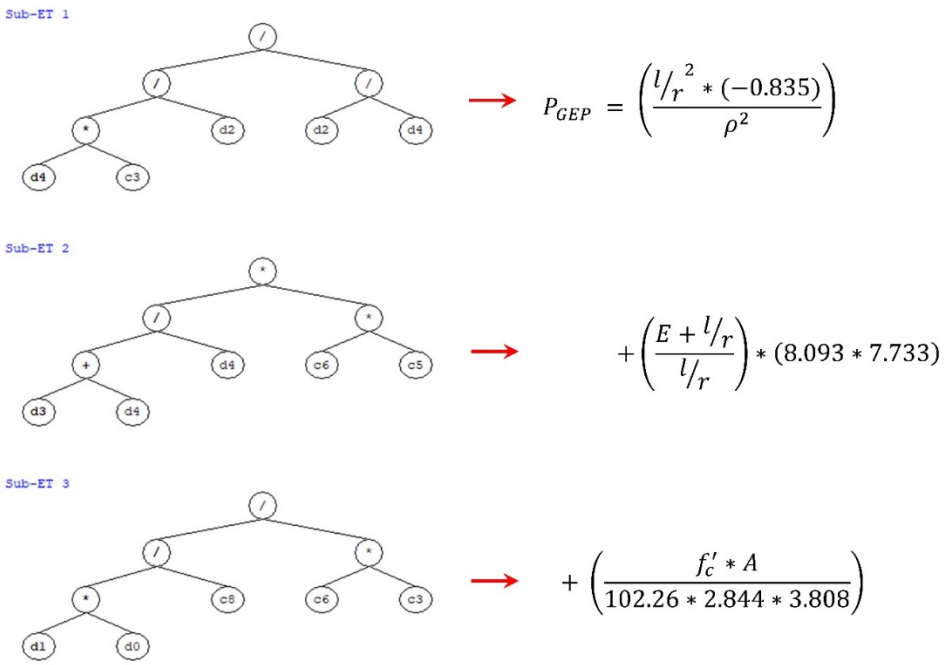

Figure 2: GEP model for concentrically loaded columns in ET format and the associated empirical equations

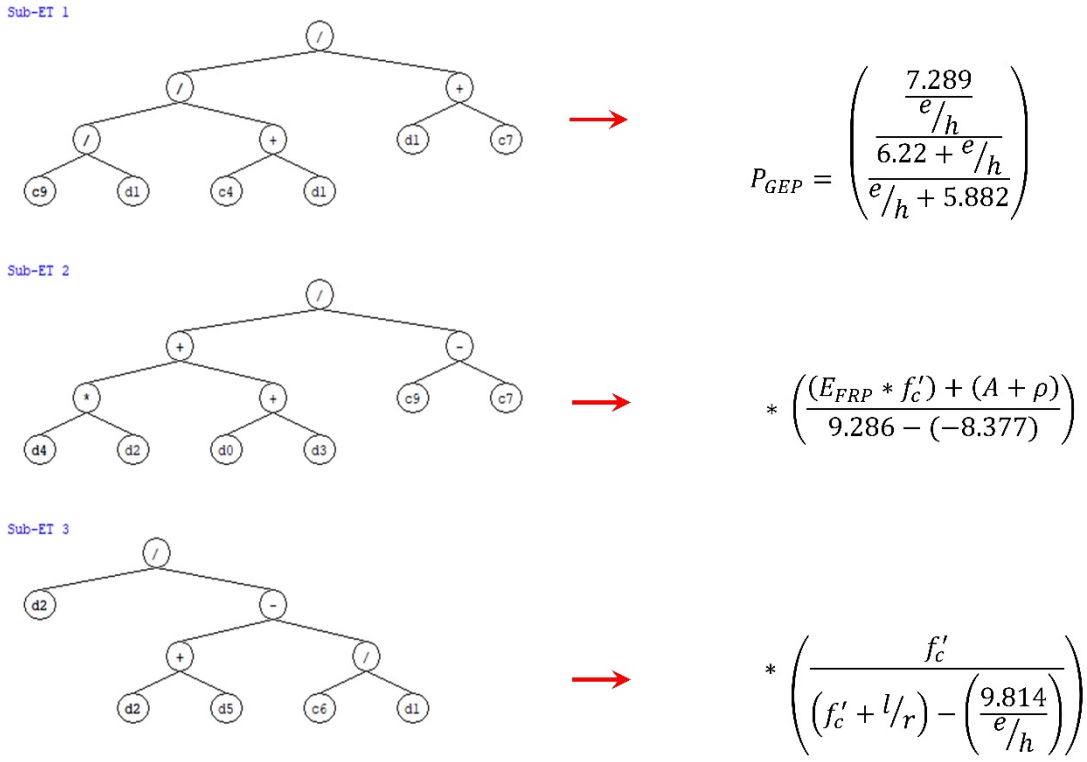

$$P_{GEP} = \left(\frac{\frac{7.289}{e/h}}{\frac{6.22 + e/h}{e/h + 5.882}} \right)$$

$$* \left(\frac{(E_{FRP} * f_c') + (A + \rho)}{9.286 - (-8.377)} \right)$$

$$* \left(\frac{f_c'}{\left(f_c' + l/r\right) - \left(\frac{9.814}{e/h}\right)} \right)$$

Figure 3: GEP model for eccentrically loaded columns in ET format and the associated empirical equation

Table 3: Constants in the GEP model

Concentric model			Eccentric model		
Sub-ET	Constant	Value	Sub-ET	Constant	Value
Sub-ET 1	G1C3	-0.835	Sub-ET 1	G1C7	5.882
Sub-ET 2	G2C5	-7.733	Sub-ET 1	G1C9	7.289
Sub-ET 2	G2C6	-8.0930	Sub-ET 1	G1C4	6.22
Sub-ET 3	G3C8	-102.26	Sub-ET 2	G2C9	9.286
Sub-ET 3	G3C6	2.844	Sub-ET 2	G2C7	-8.377
Sub-ET 3	G3C3	-3.808	Sub-ET 3	G3C6	9.814

The expression tree for each model, shown in Figs. 2 and 3, can be reformed into a mathematical equation following the procedure shown in Fig. 1, for concentric and eccentric models as follows:

$$P = \frac{-0.835(l/r)^2}{\rho^2} + \frac{62.58(E + l/r)}{l/r} + \frac{(f_c' \text{ x } A)}{1107.47} \quad (1)$$

$$P = \left(\frac{7.289}{e/h}\right)\left(\frac{e/h + 5.882}{6.22 + e/h}\right)\left(\frac{E f_c' + A + \rho}{17.663}\right)\left(\frac{f_c'}{f_c' + l/r - \frac{9.814}{e/h}}\right) \quad (2)$$

Fig. 4. shows the predicted versus experimental capacities for concentric loading (Fig. 4 (a)) and eccentric loading (Fig. 4 (b)) and the associated coefficient of determination (R^2). It can be seen that both models resulted in a high R^2. It is observed that the concentric and eccentric axial capacities estimated using the GEP models have RMSE of (231, 167.8) N, respectively, and COV of (9%, 19%), respectively, and 1.0 in terms of average axial load values ($P_{tested} / P_{predicted}$). Based on these statistical values, it is observed that the proposed models accurately predict the axial load, due to the consideration of all influencing parameters and the use of a large set of data in this study.

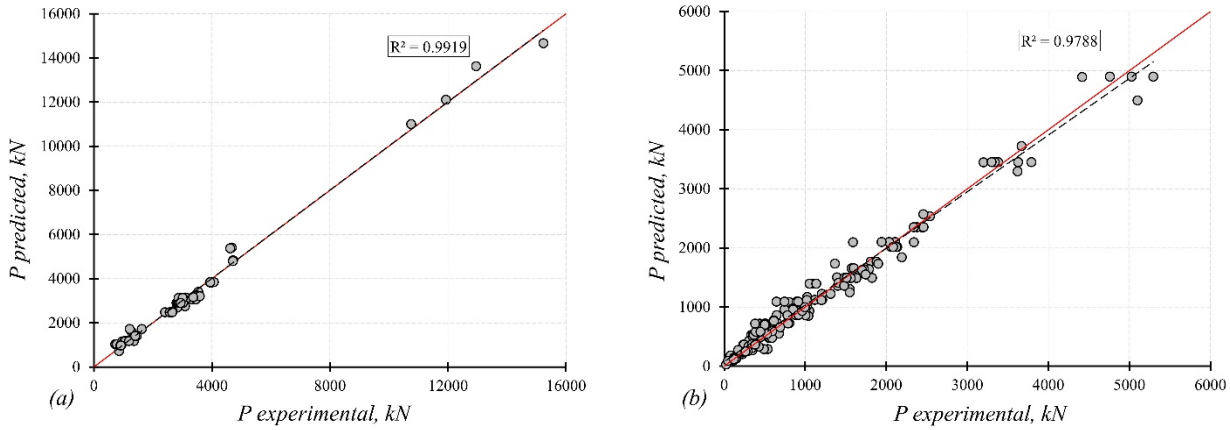

Figure 4: Correlation values of the proposed models. (a) Concentric load (b) Eccentric load.

Additionally, the model accuracy can be assessed by studying the ratio $P_{tested} / P_{predicted}$ for all affecting parameters as shown in Fig. 5 and Fig. 6. The slope of the trendline represents the consistency of the prediction with respect to each variable. The ratio of $P_{tested} / P_{predicted}$ for concentric model resulted in nearly flat slopes for all variables, which indicates consistency in prediction over all variable ranges. Regarding the eccentric loading model, the prediction also resulted in a nearly flat slope for all variables except the eccentricity level. The negative slope in Figure 6 (a) indicates an overestimation in the predicted axial strength at a high eccentricity level. It should be noted that the prediction models are only applicable within the ranges of the variables.

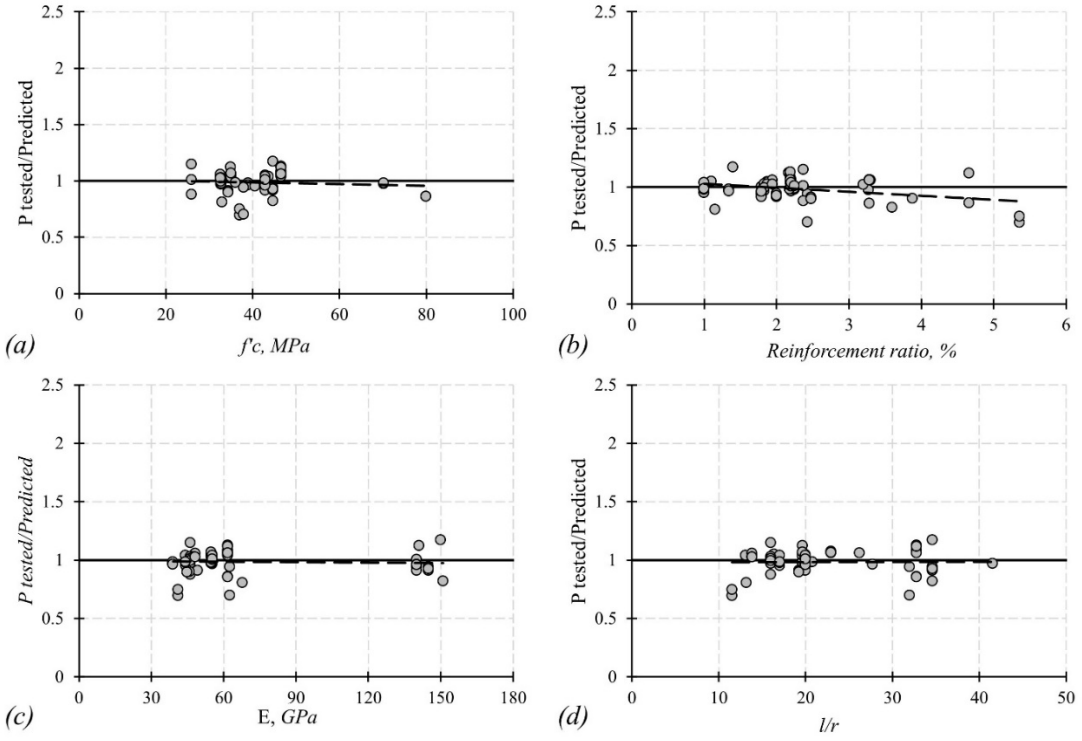

Figure 5: Accuracy of the proposed model for concentric load capacity with respect to a) $f_c^{'}$, MPa b) ρ, % c) E, GPa and d) *l/r*

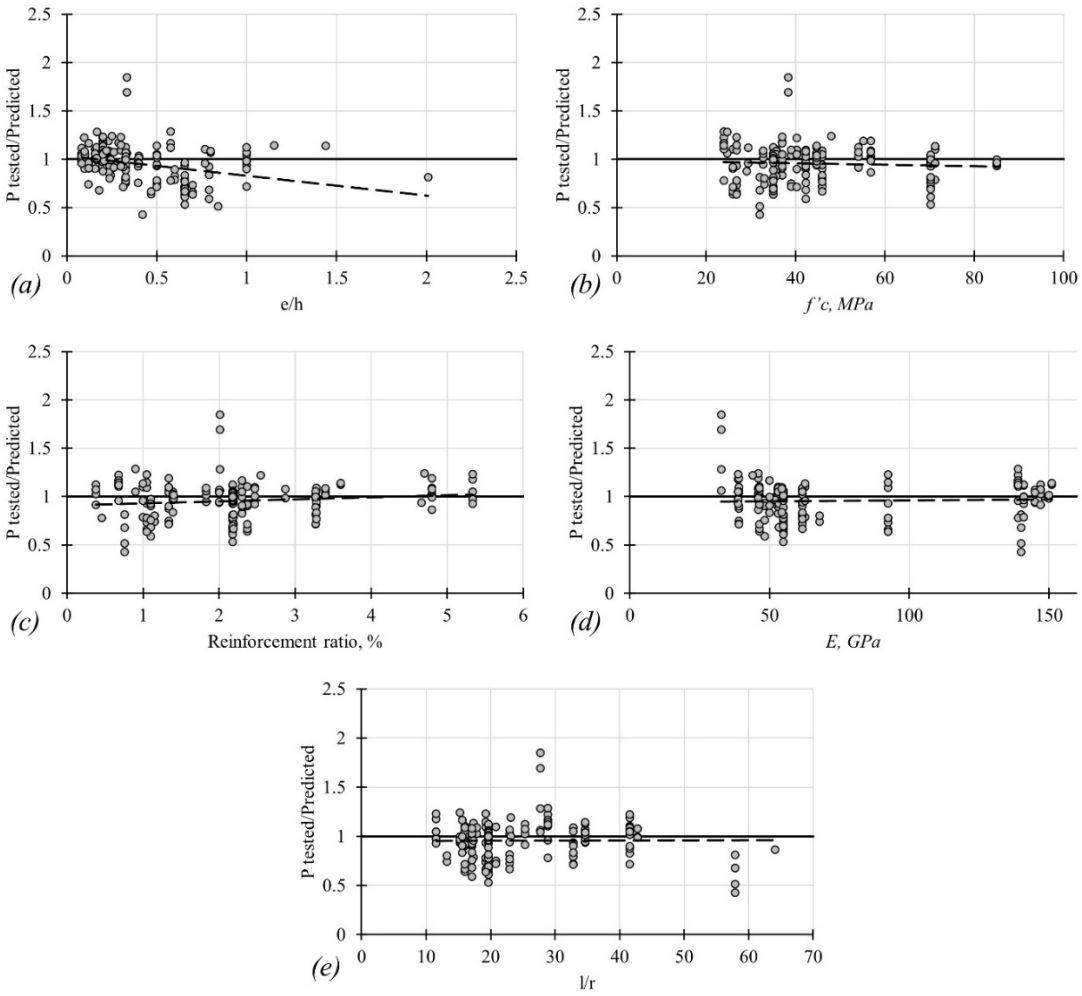

Figure 6: Accuracy of the proposed model for eccentric load capacities concerning a) e/h b) $f_c^{'}$, MPa c) ρ, % d) E, GPa e) *l/r*

4.1 Comparison with existing models

An evaluation of the proposed model prediction with respect to other existing models (Table 4) for concentrically loaded columns has been performed and shown in Figure 7. Due to the lack of proposed models in literature for eccentrically loaded columns, the comparison is carried out for concentric columns only.

The first model in comparison is adopted by the ACI 440-15 (Eq. 3) which approximates the FRP compression contribution with concrete, and accordingly, assumes the entire cross-section is concrete. This approximation is justified due to the low elastic modulus of FRP bars. The prediction model adopted by CSA-S806 neglects the FRP compression contribution as shown in Equation 6. In contrast with Equation 5, the proposed model by Mohammad et al. 2014 accounts directly for the FRP compression contribution using Hook's law with an assumed strain of 0.002 in FRP bars. The strain 0.002 had been selected as it represents the initiation of plastic deformation in concrete. Equations 6 and 7 follow a similar structure to equation 5 but with different proposed strains in FRP bars. Equation 6 assumes a strain of 0.003 in concrete and FRP bars, while equation 7 assumes 0.0035.

As expected equations 3 and 4 resulted in a higher average than other models due to neglecting FRP compression contribution. However, they resulted in a lower COV compared to other models. The proposed model by Mohammad et al. 2014 yielded the best performance among all models. In contrast, It is observed that the proposed model provided the lowest COV and RMSE. This also implies that the model was successful in learning this problem and predicting the effect of each parameter.

Table 4 Existing empirical equations for the determination of the axial capacity

$P = 0.85 f_c^{'} A_g$ Eq. (3)	ACI 440[5]
$P = 0.85 f_c^{'} (A_g - A_{FRP})$ Eq. (4)	CAN/CSA S806 [6]
$P = 0.85 f_c^{'} (A_g - A_{FRP}) + 0.002 E_{FRP} A_{FRP}$ Eq. (5)	Mohammad et al. 2014 [37]

$P_o = 0.85f_c^{'}(A_g - A_{FRP}) + 0.003E_{FRP}A_{FRP}$ Eq. (6)	ACI 318
$P_o = 0.85f_c^{'}(A_g - A_{FRP}) + 0.0035E_{FRP}A_{FRP}$ Eq. (7)	CSA-A23.3

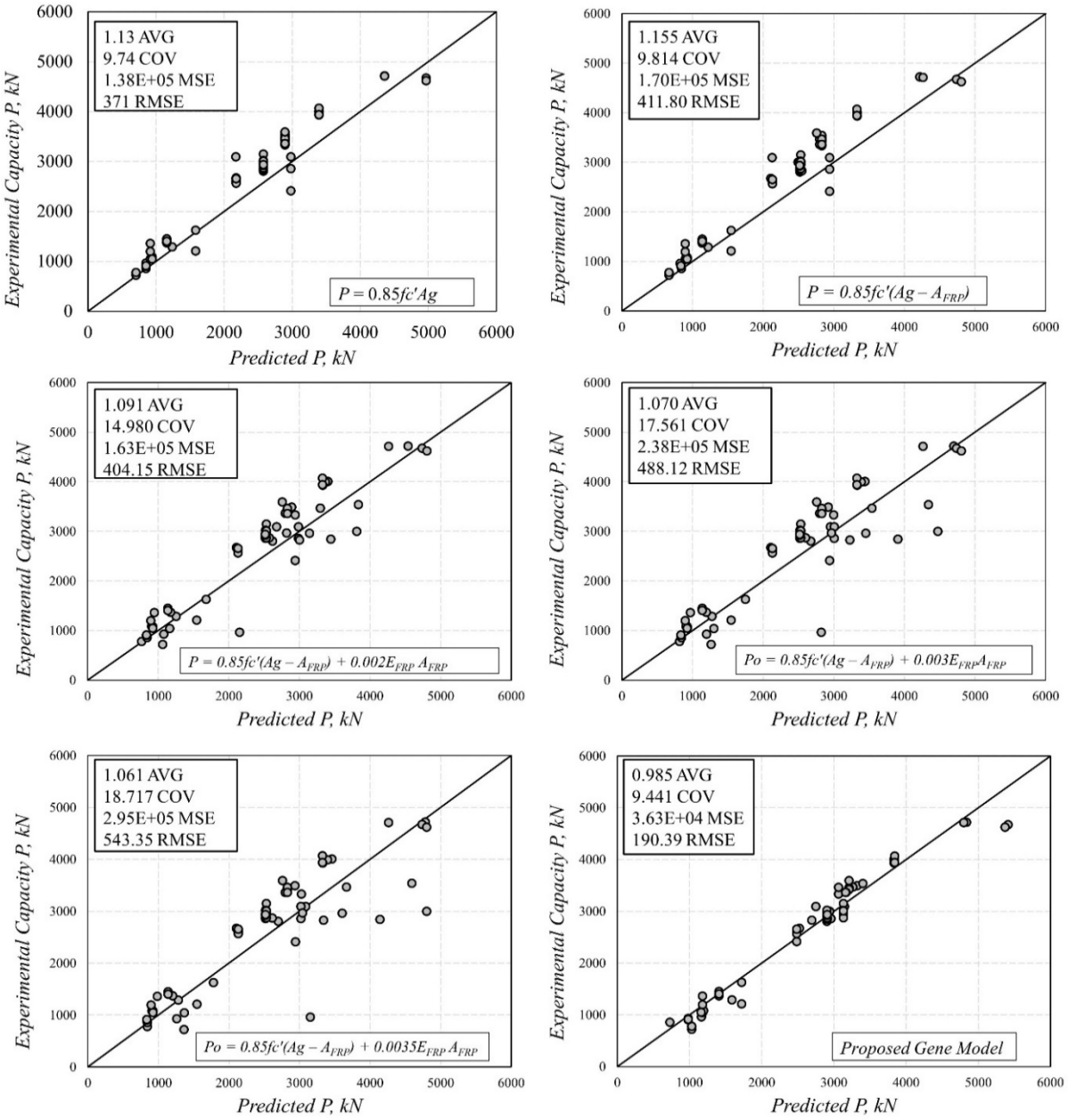

Figure 7: Comparison between the empirical equations shown in Table 3 and the proposed model

4.2 Parametric Analysis

To determine the impact of each of the model's variables discussed above on the axial capacity, a parametric analysis is carried out using the two GEP models that have been established. The 247 columns in the original database made it easier to evaluate variables with a broad range of values. The analysis is conducted by selecting one variable at a time and then assigning different values for that specific variable while keeping all other variables fixed at their average values obtained by studying the entire data set of 247 columns.

4.2.1 Effect of concrete compressive strength

Fig. 8 shows the effect of varying concrete compressive strength ($f_c^{'}$) on axial resistance for both centrally loaded columns and eccentrically loaded columns. The figure shows a strong positive correlation between increasing the concrete compressive strength and carrying load capacity. This conclusion is expected as the conducted experimental work of [Tarawneh et. al., 2022] reported a consistent concrete crushing failure mode, and no FRP bars ruptures were reported even for columns with high eccentricity [42]. This will also explain the negligible effect of FRP bars as will be shown later. Fig. 8 shows almost similar behavior for both concentric and eccentric loads.

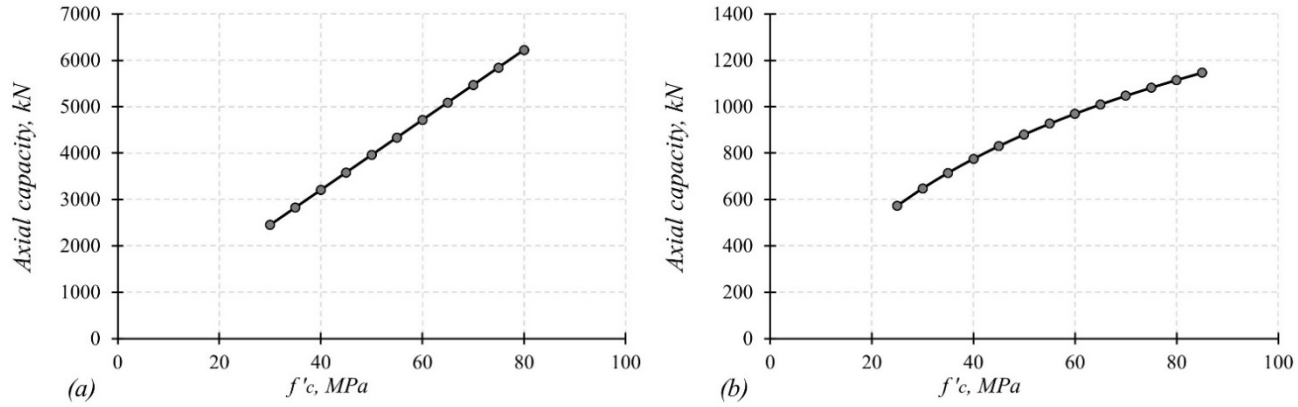

Figure 8: Effect of concrete compressive strength ($f_c^{'}$) on the predicted axial load capacity (a) Concentric load (b) Eccentric load

4.2.2 Effect of FRP elastic modulus

The effect of changing the FRP elastic modulus (E) on the axial load capacity for both concentrically and eccentrically loaded columns is shown in **Fig. 9**. An increment of the FRP elastic modulus equal to 50 MPa is used during the investigation, and the results show that the FRP elastic modulus effect was insignificant, especially for the eccentric axial load.

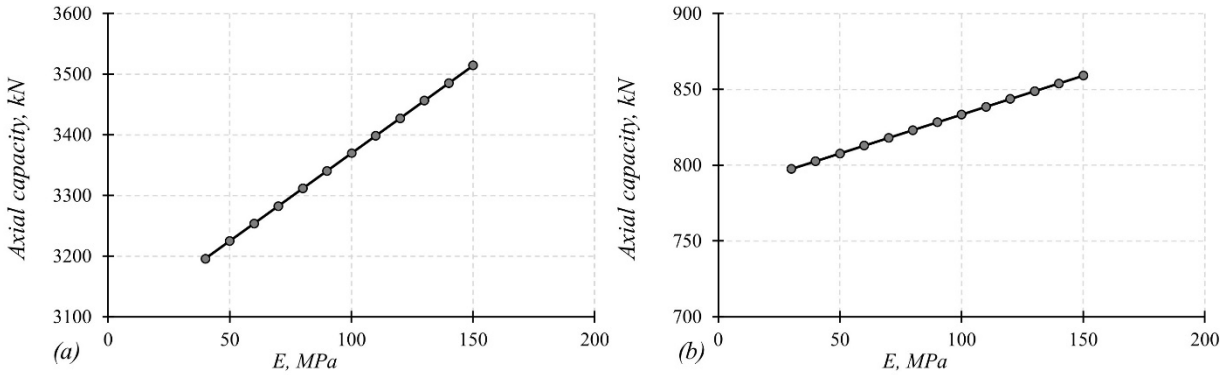

Figure 9: Effect of FRP elastic modulus (E) on the predicted axial load capacity (a) Concentric load (b) Eccentric load

4.2.3 Effect of reinforcement ratio

The effect of the reinforcement ratio (ρ) on the axial load capacity for both concentrically and eccentrically loaded columns is seen in Fig. 10. The influence of changing the column reinforcement ratio was different depending on load type. For concentric loading, the effect of the reinforcement ratio (Fig. 10a) decreases with increasing the reinforcement ratio. On the other hand, the reinforcement ratio in the eccentrically loaded column is negligible. The model ignores the reinforcement ratio effect in the eccentrically loaded column as its contribution is minimal compared to the concrete compressive strength, FRP elastic modulus, slenderness ratio, and eccentricity level as shown later

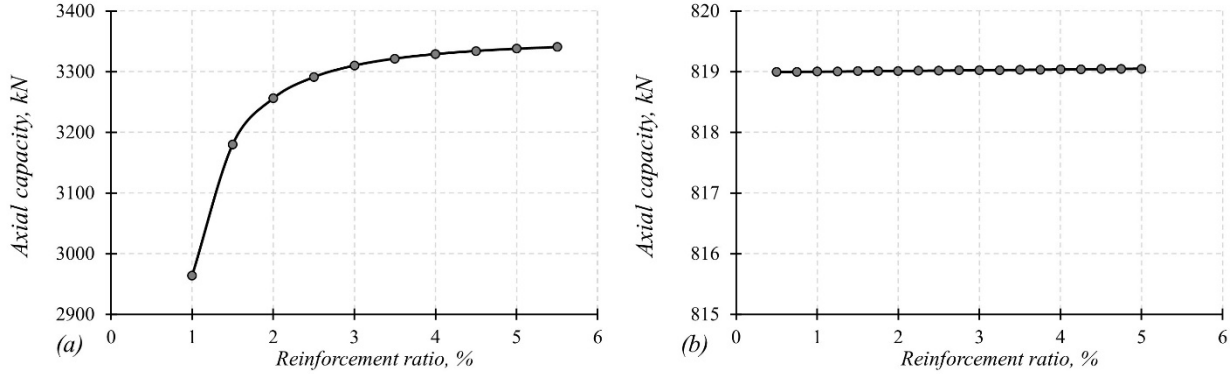

Figure 10: Effect of the reinforcement ratio (ρ) on the predicted axial load capacity (a) Concentric load (b) Eccentric load

4.2.4 Effect of slenderness ratio

Fig. 11 shows the influence of varying the slenderness ratio (*l*/*r*) on the axial load capacity for both concentrically and eccentrically loaded columns. The figure shows that the axial load capacity decrease as the slenderness ratio is increased.

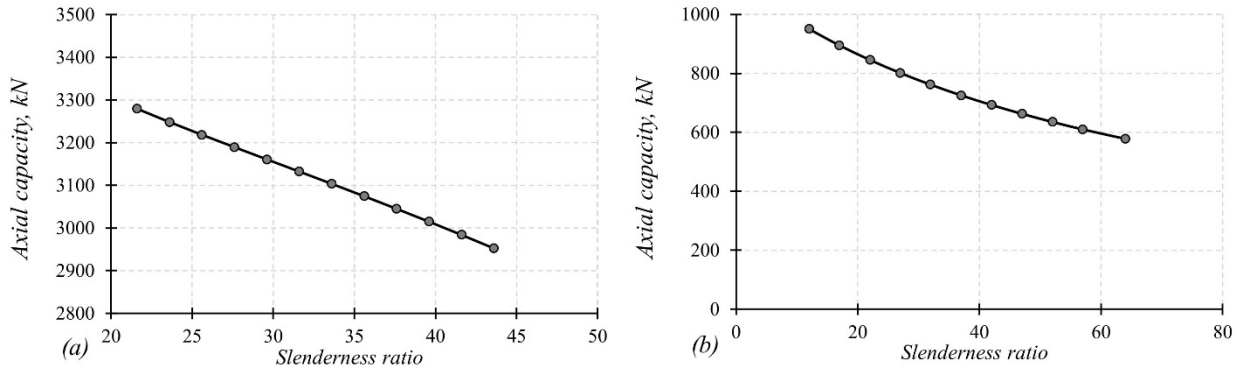

Figure 11: Effect of the slenderness ratio (*l*/*r*) on the predicted axial load capacity (a) Concentric load (b) Eccentric load

4.2.5 Effect of eccentricity level

Fig. 12 shows the influence of varying the eccentricity level (e / h) on the axial load capacity for the eccentric axial loads. As shown in Fig. 12, the capacity is dramatically influenced by the eccentricity level with nonlinear relation.

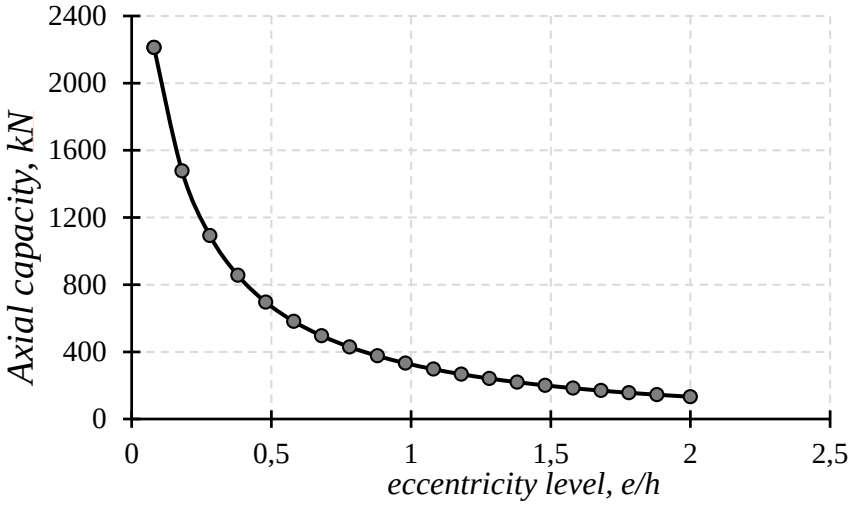

Figure 12: Effect of the eccentricity level (e / h) on the predicted eccentric axial load capacity.

5 MODEL LIMITATION AND RECOMMENDATION

Although the proposed model yielded a higher accuracy compared to other proposed procedures, data-driven machine learning models are only valid within the range of variables used to develop the models and should not be used for cases outside the range. Therefore, it is recommended to reexamine the proposed model with a larger database and a wider range of variables to validate its applicability.

6 CONCLUSIONS

In this study, gene expression programming is utilized with a database of 247 tested FRP-RC columns to generate prediction models for the axial capacity of concentrically and eccentrically loaded columns. The prediction models are applicable for concentric and eccentric loading, short and slender columns, different types of FRP reinforcement, and circular and rectangular cross-sections. In order to evaluate the sensitivity of each influencing parameter, a parametric study was also conducted. The variables taken into consideration are the concrete cylinder compressive strength, longitudinal reinforcement ratio, FRP modulus of elasticity, eccentricity ratio, and column dimensions. The following conclusions are made:

1. Two prediction models for the axial capacity of concentrically and eccentrically FRP-RC columns were developed using the GEP algorithm. The concentric and eccentric axial capacity models have RMSE of (231, 167.8) N, and COV of (9%, 19%), respectively, and 1.0 average axial load values ($P_{tested} / P_{predicted}$) for both models. in addition, The proposed models exhibited a close agreement with the experimental

database, with a coefficient of determination R^2 = 0.978 and R^2 = 0.992, for eccentric and concentric axial loads, respectively. The concentric axial load model is fed by five given inputs, which are A , E , ρ , *l/r*, and $f_c^{'}$, to predict the axial load capacity. While the eccentric load model is fed by six given inputs, which are A , E , ρ , *l/r*, e/h , and $f_c^{'}$.

2. By comparing the existing models, the ACI 440-15 equation approximates the FRP compression contribution with concrete, and accordingly, assumes the entire cross-section is concrete while the CSA-S806 equation neglects the FRP compression contribution. However, the proposed model by Mohammad et al. 2014 accounts directly for the FRP compression contribution using Hook's law with an assumed strain of 0.002 in FRP bars. As expected equations 3 and 4 resulted in a higher average than other models due to neglecting FRP compression contribution. However, they resulted in a lower COV compared to other models. In contrast, It is observed that the proposed model provided the lowest COV and RMSE.
3. Based on the parametric study performed in this study, it shows a strong positive correlation between increasing the concrete compressive strength and the carrying load capacity. The results also show that the FRP elastic modulus effect was insignificant, especially for the eccentric axial load. In addition, the effect of the reinforcement ratio decreases with increasing the reinforcement ratio for concentric loading while the reinforcement ratio in the eccentrically loaded column is negligible. The axial load capacity decrease as the slenderness ratio is increased. As shown before the capacity is significantly influenced by the eccentricity level with nonlinear relation.

7 REFERENCES

[1] Tarawneh, A., Almasabha, G. and Murad, Y., (2022). ColumnsNet: Neural Network Model for Constructing Interaction Diagrams and Slenderness Limit for FRP-RC Columns. Journal of Structural Engineering, 148(8), p.04022089.

[2] Peng, F., & Xue, W. (2019). Reliability Analysis of Eccentrically Loaded Concrete Rectangular Columns Reinforced with Fiber-Reinforced Polymer Bars. ACI Structural Journal, 116(4).

[3] Salah-Eldin, A., Mohamed, H. M., & Benmokrane, B. (2019). Structural performance of high-strength-concrete columns reinforced with GFRP bars and ties subjected to eccentric loads. Engineering Structures, 185, 286-300.

[4] Peng, F. and Xue, W., 2019. Reliability Analysis of Eccentrically Loaded Concrete Rectangular Columns Reinforced with Fiber-Reinforced Polymer Bars. ACI Structural Journal, 116(4), pp.275-284.

[5] ACI Committee 440, 2015, "Guide for the Design and Construction of Structural Concrete Reinforced with FRP Bars (ACI 440.1R-15)," American Concrete Institute, Farmington Hills, MI, 83 pp.

[6] Canadian Standards Association (CSA), 2012, "Design and Construction of Building Components with Fiber Reinforced Polymers (CAN/CSAS806-12)," CSA Group, Rexdale, ON, Canada, 208 pp.

[7] De Luca, A.; Matta, F.; and Nanni, A., "Behavior of Full-Scale Glass Fiber-Reinforced Polymer Reinforced Concrete Columns under Axial Load," ACI Structural Journal, V. 107, No. 5, Sept.-Oct. 2010, pp. 589-596

[8] Alsayed, S. H.; Al-Salloum, Y. A.; Almusallam, T. H.; and Amjad, M. A., "Concrete Columns Reinforced by GFRP Rods," Fourth International Symposium on Fiber-Reinforced Polymer Reinforcement for Reinforced Concrete Structures, SP-188, C. W. Dolan, S. H. Rizkalla, and A. Nanni, eds., American Concrete Institute, Farmington Hills, MI, 1999, pp. 103-112.

[9] Elchalakani, M., and Ma, G., 2017, "Tests of Glass Fibre Reinforced Polymer Rectangular Concrete Columns Subjected to Concentric and Eccentric Axial Loading," Engineering Structures, V. 151, pp. 93-104. doi: 10.1016/j.engstruct.2017.08.023

[10] Hadhood, A.; Mohamed, H. M.; and Benmokrane, B., 2017, "Axial Load-Moment Interaction Diagram of Circular Concrete Columns Reinforced with CFRP Bars and Spirals: Experimental and Theoretical Investigations," Journal of Composites for Construction, ASCE, V. 21, No. 2, Apr., p. 04016092 doi: 10.1061/(ASCE)CC.1943-5614.0000748

[11] Tobbi, Hany, Farghaly, Ahmed Sabry, & Benmokrane, Brahim. (2012). Concrete Columns Reinforced Longitudinally and Transversally with Glass Fiber-Reinforced Polymer Bars. *ACI Structural Journal*, *109*(4). https://doi.org/10.14359/51683874

[12] Afifi, M. Z., Mohamed, H. M., & Benmokrane, B. (2014). Axial Capacity of Circular Concrete Columns Reinforced with GFRP Bars and Spirals. Journal of Composites for Construction, 18(1), 04013017. https://doi.org/10.1061/(ASCE)CC.1943-5614.0000438

[13] Guérin, M.; Mohamed, H. M.; Benmokrane, B.; Nanni, A.; and Shield, C. K., 2018a, "Eccentric Behavior of Full-Scale Reinforced Concrete Columns with Glass Fiber-Reinforced Polymer Bars and Ties," ACI Structural Journal, V. 115, No. 2, Mar., pp. 489-499. doi: 10.14359/51701107.

[14] Guérin, M.; Mohamed, H. M.; Benmokrane, B.; Shield, C. K.; and Nanni, A., 2018b, “Effect of Glass Fiber-Reinforced Polymer Reinforcement Ratio on Axial-Flexural Strength of Reinforced Concrete Columns,” *ACI Structural Journal*, V. 115, No. 4, July, pp. 1049-1061. doi: 10.14359/51701279

[15] Raza, A., Shah, S. A. R., ul Haq, F., Arshad, H., Raza, S. S., Farhan, M., & Waseem, M. (2020, December). Prediction of axial load-carrying capacity of GFRP-reinforced concrete columns through artificial neural networks. In Structures (Vol. 28, pp. 1557-1571). Elsevier.

[16] Kisi, Ö., & Çobaner, M. (2009). Modeling River Stage-Discharge Relationships Using Different Neural Network Computing Techniques. CLEAN - Soil, Air, Water, 37(2), 160–169. https://doi.org/10.1002/clen.200800010

[17] Solhmirzaei, R., Salehi, H., Kodur, V. and Naser, M.Z., 2020. Machine learning framework for predicting failure mode and shear capacity of ultra-high performance concrete beams. Engineering structures, 224, p.111221.

[18] Tarawneh, A., Almasabha, G., Alawadi, R. and Tarawneh, M., 2021, August. Innovative and reliable model for shear strength of steel fibers reinforced concrete beams. In Structures (Vol. 32, pp. 1015-1025). Elsevier.

[19] Imam, R., Murad, Y., Asi, I. and Shatnawi, A., 2021. Predicting pavement condition index from international roughness index using gene expression programming. Innovative Infrastructure Solutions, 6(3), pp.1-12.

[20] Xue, W.; Peng, F.; and Fang, Z., 2018, “Behavior and Design of Slender Rectangular Concrete Columns Longitudinally Reinforced with Fiber-Reinforced Polymer Bars,” ACI Structural Journal, V. 115, No. 2, Mar., pp. 311-322. doi: 10.14359/51701131

[21] Amer, A.; Arockiasamy, M.; and Shahawy, M., 1996, “Ultimate Strength of Eccentrically Loaded Concrete Columns Reinforced with CFRP Bars,” Proceedings of the Conference on Advanced Composite Materials in Bridges and Structures, Montreal, QC, Canada, pp. 209-216.

[22] Sharbatdar, M. K., 2003, “Concrete Columns and Beams Reinforced with FRP Bars and Grids under Monotonic and Reversed Cyclic Loading,” PhD dissertation, University of Ottawa, Ottawa, ON, Canada, 371 pp.

[23] Tikka, T. K.; Francis, M.; and Teng, B., 2010, “Strength of Concrete Beam Columns Reinforced with GFRP Bars,” 2nd International Structures Specialty Conference, Winnipeg, MB, Canada, pp. 1194-1203.

[24] Gong, Y.; and Zhang, J., 2009, “Experimental Study of Reinforced Concrete Eccentric Compression Columns with CFRP Tendons,” China Civil Engineering Journal, V. 42, No. 10, Oct., pp. 46-52. (in Chinese) doi:10.15951/j.tmgcxb.2009.10.012

[25] Elchalakani, M.; Karrech, A.; Dong, M.; Ali, M.; and Yang, B., 2018, “Experiments and Finite Element Analysis of GFRP Reinforced Geopolymer Concrete Rectangular Columns Subjected to Concentric and Eccentric Axial Loading,” Structures, V. 14, June, pp. 273-289. doi: 10.1016/j.istruc.2018.04.001

[26] Khorramian, K., and Sadeghian, P., 2017, “Experimental and Analytical Behavior of Short Concrete Columns Reinforced with GFRP Bars under Eccentric Loading,” Engineering Structures, V. 151, Nov, pp. 761-773. doi: 10.1016/j.engstruct.2017.08.064

[27] Sun, L.; Wei, M.; and Zhang, N., 2017, “Experimental Study on the Behavior of GFRP Reinforced Concrete Columns under Eccentric Axial Load,” Construction and Building Materials, V. 152, Oct., pp. 214-225. doi: 10.1016/j.conbuildmat.2017.06.159

[28] Issa, M.S., Metwally, I.M. and Elzeiny, S.M., 2011. Structural performance of eccentrically loaded GFRP reinforced concrete columns. International Journal of Civil & Structural Engineering, 2(1), pp.395-406.

[29] Othman, Z.S. and Mohammad, A.H., 2019. Behaviour of Eccentric Concrete Columns Reinforced with Carbon Fibre-Reinforced Polymer Bars. Advances in Civil Engineering, 2019.

[30] Salah-Eldin, A., Mohamed, H.M. and Benmokrane, B., 2019. Structural performance of high-strength-concrete columns reinforced with GFRP bars and ties subjected to eccentric loads. Engineering Structures, 185, pp.286-300.

[31] Hadi, M.N., Karim, H. and Sheikh, M.N., 2016. Experimental investigations on circular concrete columns reinforced with GFRP bars and helices under different loading conditions. Journal of Composites for Construction, 20(4), p.04016009.

[32] Khorramian, K. and Sadeghian, P., 2019, April. Behavior of Slender GFRP Reinforced Concrete Columns. In ASCE-SEI Structures Congress 2019. American Society of Civil Engineers.

[33] Abdelazim, W., Mohamed, H. M., Benmokrane, B., & Afifi, M. Z. (2020). Effect of critical test parameters on behavior of glass fiber-reinforced polymer-reinforced concrete slender columns under eccentric load. ACI Structural Journal, 117(4), 127-141.

[34] Khorramian, K., & Sadeghian, P. (2020). Experimental Investigation of Short and Slender Rectangular Concrete Columns Reinforced with GFRP Bars under Eccentric Axial Loads. Journal of Composites for Construction, 24(6), 04020072.

[35] Maranan, G. B., Manalo, A. C., Benmokrane, B., Karunasena, W., & Mendis, P. (2016). Behavior of concentrically loaded geopolymer-concrete circular columns reinforced longitudinally and transversely with GFRP bars. Engineering Structures, 117, 422-436.

[36] Elmesalami, N., Abed, F., & Refai, A. E. (2021). Concrete columns reinforced with GFRP and BFRP bars under concentric and eccentric loads: Experimental testing and analytical investigation. Journal of Composites for Construction, 25(2), 04021003.

[37] Mohamed, H. M.; Afifi, M. Z.; and Benmokrane, B., "Performance Evaluation of Concrete Columns Reinforced Longitudinally with FRP Bars and Confined with FRP Hoops and Spirals under Axial Load," Journal of Bridge Engineering, ASCE, V. 19, No. 7, 2014, p. 04014020. doi: 10.1061/(ASCE)BE.1943-5592.0000590.

Paper submitted: 20.08.2022.

Paper accepted: 06.11.2022.